Resources, Conservation & Recycling 131 (2018) 192–205

Contents lists available at ScienceDirect

Resources, Conservation & Recycling

journal homepage: www.elsevier.com/locate/resconrec

Full length article

Performance evaluation of material separation in a material recovery facility using a network flow model

Karine Ip[a,*], Mariapaola Testa[b], Anne Raymond[a], Stephen C. Graves[b], Timothy Gutowski[a]

[a] Department of Mechanical Engineering, Massachusetts Institute of Technology, 77 Massachusetts Ave, Cambridge, MA 02139, United States
[b] Sloan School of Management, Massachusetts Institute of Technology, 77 Massachusetts Ave, Cambridge, MA 02139, United States

ARTICLE INFO

Keywords:
Material separation
Recycling
Network flow model
Model parameter estimation

ABSTRACT

In this paper, we model the recycling process for solid waste as performed in a material recovery facility. The intent is to inform the design and evaluation of a material recovery facility (MRF) in order to increase its profit, efficiency and recovery rate. We model the MRF as a multi-stage material separation process and develop a network flow model that evaluates the performance of the MRF through a system of linear equations. We estimate the parameters of the network flow model from historical data to find the best fit. We validate the model using a case-study of a light-packaging recovery section of an MRF in Spain. Additionally, we examine how uncertainty in the input material composition propagates through the system, and conduct a sensitivity analysis on the model parameters.

1. Introduction

Recycling is a major element of integrated solid waste management (SWM) in developed countries. Recycling of solid waste is a preferred option relative to landfill and incineration, due to the rapid depletion of landfill space and air pollution emissions from incineration (Chang and Pires, 2015). Furthermore, recycling permits the recovery of valuable raw materials. Consequently, many countries have enacted national and regional waste legislation that require recycling, such as the Resource Conservation and Recovery Act which implements the Sustainable Materials Management Program in the United States (Chang and Pires, 2015). In Spain, the Waste Framework Directive sets a target for Spain to recycle 50% of its municipal solid waste by 2020 (Milios and Reichel, 2013). A recycling program can differ in its collection method (single, dual or multi-stream). In this research we consider the collected municipal waste, which is processed at a material recovery facility (MRF). The MRF is a system of mechanical and manual separation processes that sorts the multi-stream waste to recover recyclable materials. MRFs in the US and Spain are facing challenges due to volatile scrap market prices (e.g. for plastic waste (Ragaert et al., 2017)) as well as changing scrap buyer requirements. The latter challenge stems from China's Operation Green Fence. Since 2013, China, a major importer of recyclable waste, turns away recyclable materials that fail to meet stricter contaminant levels (Gu et al., 2017). Another challenge is the variability in the composition of the waste streams received by the MRFs. To address these challenges, it is crucial that MRFs understand how their operating performance depends on the scrap-market prices and quality requirements, as well as on the waste input streams. This understanding can allow the MRFs to examine adaptation strategies in light of the scrap market dynamics and input variability. In this paper we develop and test a network flow model for an MRF. The intent of the model is to provide a tool for predicting the performance of an MRF, and for showing how this performance depends on the configuration and parameters of the system, and on the input materials. Potential applications include cost-benefit analyses of modifications to the design and operation of an MRF; for instance, these modifications might increase the recovery or grade of a profitable material.

The material recovery model developed in this paper will contribute to furthering the development of a circular economy. The model allows for the determination of the material recovery rate and grade from a municipal waste input stream, and can be used to identify system improvements that both increase the quantity and/or quality of the valuable recovered materials, as well as reduce the amount lost to landfills. Whereas this model has been developed for a municipal waste application, it should also apply to other material recovery systems that use similar separation technologies. For instance, we expect that the model, with some adaptation, can be applied to the separation step in the recovery system for end-of-life vehicles, which comes after the dismantling and shredding steps.

* Corresponding author.
E-mail address: karineip@mit.edu (K. Ip).

https://doi.org/10.1016/j.resconrec.2017.11.021
Received 29 December 2016; Received in revised form 23 November 2017; Accepted 25 November 2017
Available online 12 January 2018
0921-3449/

1.1. Literature review

Solid waste recycling is part of the larger framework of waste management, which examines the flow of waste from generation in rural or urban settings to treatment, recovery or disposal. There is an extensive literature on waste management. In particular, we cite the research that focuses on decision-making processes, namely capacity-planning of facilities for treatment and material recovery, routing systems for waste collection, and resource allocation (Antmann et al., 2013; Chang et al., 2005; Huang et al., 2005; Shi et al., 2014). Additionally, we mention the research that includes environmental considerations. For plastic waste management, Rigamonti et al. (2014) look at different collection-routing strategies from an energy recovery perspective, while Shonfield (2008) carries out a life cycle assessment (LCA) study of a range of plastic recycling technologies. Gaustad et al. (2012) examine the environmental and economic impact of various technologies used for aluminum recycling. Kirkeby et al. (2006) examine the LCA of material flows using EASEWASTE, a computational model tool developed for this purpose. Several papers rely on estimated parameters to characterize the performance of an MRF for a particular material flow: Kirkeby et al. (2006) introduce mass transfer coefficients, parameters input by the user to characterize a material's overall recovery; Palmer (1999) and Diaz et al. (1982) use recovery factor transfer function for each material flow in each unit in an MRF.

Material separation of collected waste is carried out mechanically in MRFs based on the physical properties of each material. For instance, aluminum materials are sorted by virtue of their electrical conductivity using eddy-current separation equipment (Braam et al., 1988; Schloemann, 1982). Ferrous materials are sorted by magnet separators in pulley, drum or belt form (UNEP, 2005). Glass and plastic (including HDPE, PET and Tetrabrik) are separated from other materials by detect-and-route systems, whereby sensors detect target materials and air jets divert the localized objects (Stressel, 2012). Sensors using spectroscopic near-infrared (NIR) imaging have been shown to successfully sort between different types of plastics after training with statistical pattern recognition techniques (Van Den Broek et al., 1997). Huang investigated the use of optical sensors for multi-feature recognition of different waste mixtures (Huang et al., 2010). MRFs also carry out separation based on particle properties at the start of the system configuration: screening, usually done with trommels, separates based on object size (Stressel, 2012; UNEP, 2005); ballistic separators distinguish between flat, light items (e.g., paper, films) and heavy, rigid items (e.g., containers) based on particle elasticity and aerodynamic properties (Hershaft, 1972; Testa, 2015). In addition to automated sorting technologies as described above, manual sorting is also used in some MRFs. For instance, personnel in sorting stations situated before the trommels collect large-size objects while those in stations before the final baling of the plastics and aluminum output streams remove non-valuable waste (Stressel, 2012; UNEP, 2005).

MRFs sort materials using a sequence of separation processes. Beyond an understanding of the physical process for each separation unit, we need to model all the units as a connected network. Modeling of a network of material separation processes has been carried out in other fields, most specifically in mineral processing (Mckeon and Luttrel, 2012; Noble and Luttrell, 2014a,b). These papers use a linear circuit analysis approach, with the separation function defined for different separation technologies based on physical properties. In (Dahmus and Gutowski, 2007; Gutowski et al., 2008, 2007), a similar approach, called 'Bayesian separation', is introduced to define material separation models from a probabilistic point of view. The probabilities for correct routing of target material and non-target material are also defined. Vanegas et al. (2015) use this approach to model the recycling of LCD TVs.

Several papers have studied the costs and operations of an MRF in various contexts: Metin et al. estimated the investment and operating costs of different municipal MRFs in Turkey using city-wide aggregate data (Metin et al., 2003); Kang and Schoenung examined the cost drivers of an existing e-waste MRF (Kang and Schoenung, 2006); Li et al. considered how sorting strategies can impact the utilization of scrap in a secondary aluminum production process. (Li et al., 2011). However, these papers do not model the material flows through the individual separation units, but rather assume a given material recovery rate. There is limited literature concerning the actual design optimization of the network of separation processes used in MRFs. Wolf (Wolf, 2011; Wolf et al., 2013), and Testa (Testa, 2015) provide the groundwork for the development of a network flow model which can represent an MRF with multiple output units and recirculating streams. In this paper, we formulate a network flow model for an MRF as done in these prior works, provide an approach for parameter estimation and present a case study illustrating the model.

2. Mathematical model

The aim of the mathematical model is to represent the material separation processes in terms of the mass flow of material in a network of sorting units that includes recirculation loops. We assume a stationary flow of input material, and no build-up or buffering of any of the flows in the MRF.

We model each separation process on a per material basis, with an empirically-derived separation (or efficiency) parameter which quantifies the fraction of a material sent to each output stream of a sorting unit. We do not attempt a physical modeling of the sorting units; such models are rarely available for a whole MRF network (Chang and Pires, 2015). Future work could incorporate the physical parameters of the sorting unit that determine its separation efficiency (e.g. height of the magnet, strength of the current) by making the separation efficiency a function of these physical parameters.

As the building block for the network model, we consider a multi-output sorting unit that sorts a mixture of M materials into K output streams. For each material m, we define a mass flow rate of f_i^m in the input stream (e.g., ton per hour) to unit i. The sorting unit will separate this material input into K output streams. The mass flow in the output stream k is $q_{i,k}^m f_i^m$, where $q_{i,k}^m$ is the fraction of the input stream of material m that is sorted into output stream k by unit i. $q_{i,k}^m$ is called the separation parameter. Consequently we have $\sum_{k=1}^{K} q_{i,k}^m = 1$. Fig. 1 shows the most common case when there are only $K = 2$ output streams: if unit i sorts for target material type (m = T), it diverts a fraction of its flow, denoted by $q_{i,j}^{\mathrm{T}}$, to target unit j, and diverts $q_{i,k}^{N}$ of the flow of non-target material type(s) (m = N) to non-target unit k. $q_{i,j}^{\mathrm{T}}$ and $q_{i,k}^{\mathrm{N}}$ are expected to be greater than 0.5.

We use this building block to develop the mathematical model for an MRF. An MRF can be represented as a network of multi-output units, as shown in Fig. 2. We model the system configuration with three types of units: a set I of input nodes, a set S of sorting units and a set Z of output nodes. Each input node feeds an input stream to an initial sorting unit. The input to each sorting unit can consist of an input stream from an input node, plus the output streams from other sorting

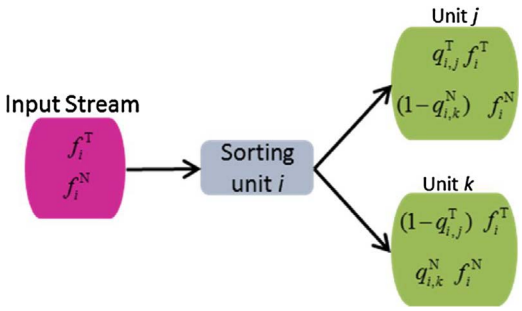

Fig. 1. Scheme of a multi-output unit sorting an input mixture of target and non-target materials into 2 streams.

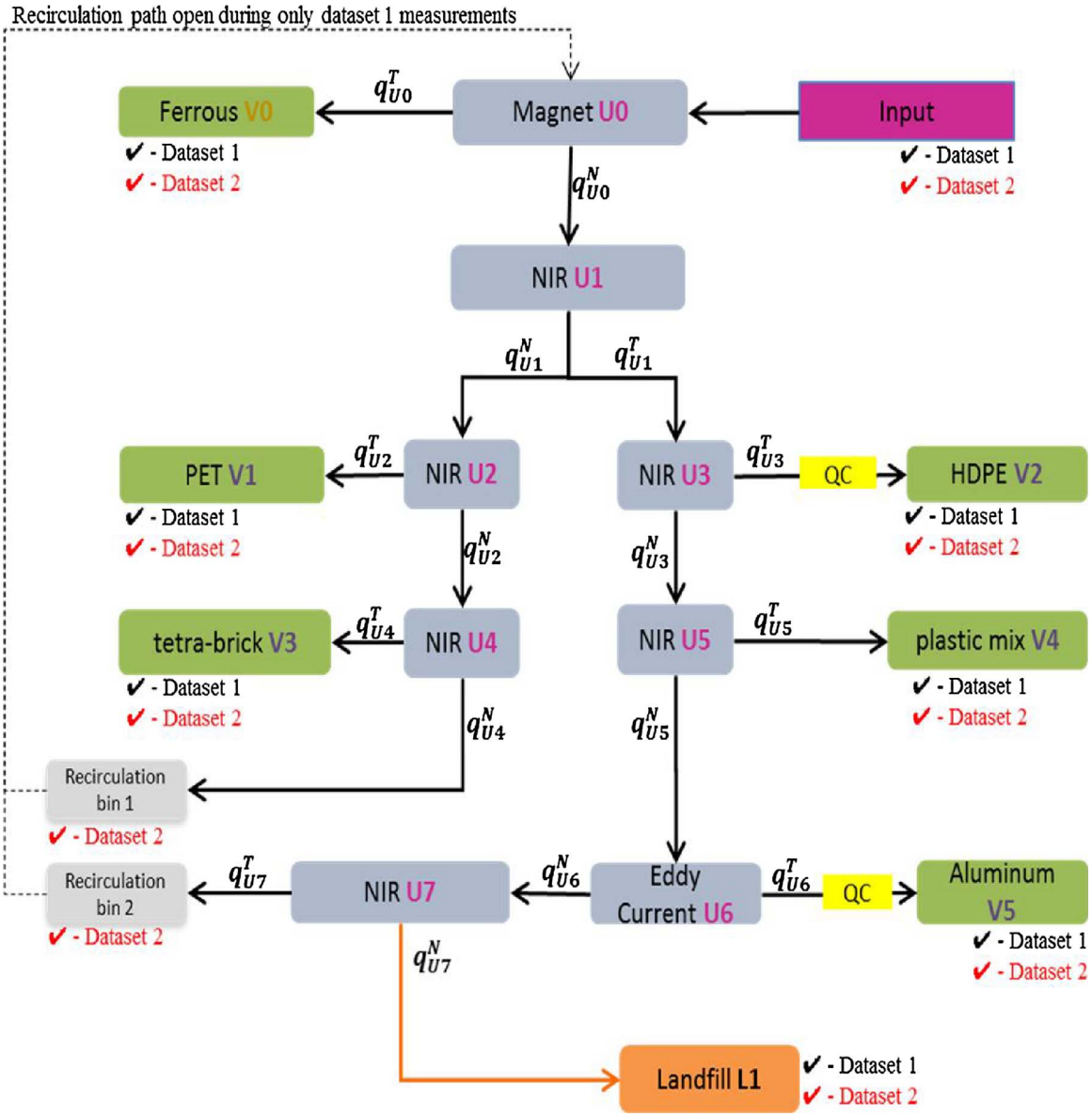

Fig. 2. Schematic of LPRS, showing datasets for separation parameter estimation.

units. Each sorting unit can generate multiple output streams as described above. The input to the output nodes can come from one or more sorting units. There is no output flow from an output node, as it represents a collection unit for the MRF (Testa, 2015).

We can write the mass-balance equation for the flow of each material through each sorting and output unit j as follows:

$$f_j^m = \mu_j^m + \sum_i q_{i,j}^m f_i^m \tag{1}$$

with f_i^m, $q_{i,j}^m$ defined previously and μ_j^m being the external input rate of material m to unit j. We note that $q_{i,j}^m = 0$ if there is not a direct connection between unit i and j; and we have $\mu_j^m \neq 0$ only if there is an input unit that feeds sorting unit j. For each material m, we can write (1) as a system of linear equations (Testa, 2015):

$$\overline{f}^m = \overline{\mu}^m + (Q^m)^T \overline{f}^m \tag{2}$$

$\overline{f}^m$ is the flow vector (Nx1) for material m, with elements f_i^m. $\overline{\mu}^m$ is the input vector (Nx1) for material m, with elements μ_i^m, Q^m is the sorting matrix (NxN) for material m, with elements $q_{i,j}^m$. N is the number of sorting units plus output units.

We can solve the system of linear Eq. (2) to obtain the steady-state flow rates for each material at each unit:

$$\overline{f}^m = (I - (Q^m)^T)^{-1} \overline{\mu}^m \tag{3}$$

We estimate the separation parameters $q_{i,j}^m$ for each connection in the MRF configuration from an empirical characterization of measurement samples (an estimation method is covered in section III). The estimated parameters may depend on the specific input composition, feed rate, and operational settings used during the measurements. For this paper, we do not consider the effects of these factors, i.e., we assume that the separation parameters are constant and independent from these factors (Testa, 2015).

We note that the separation parameters are based solely on the type of material, as many of the sorting equipment in an MRF operate based on physical material properties (e.g. magnets sort by ferrous and magnetic properties, eddy-current separators sort by metallic properties, NIRs sort by plastics' optical properties). However, some sorting units sort by shape and size (e.g., trommels), or by shape and density (e.g., ballistic separators). Note that the separation parameters $q_{i,j}^m$ do not explicitly consider material characteristics other than material type (e.g., shape, size or density). Testa (2015) demonstrates how to extend the modeling framework to accommodate sorting units that sort by

material shape and size.

In addition to mechanical sorting units, MRFs may include manual operations: hand-sorting (HS) cabins and quality-control (QC) units. In the hand-sorting cabins, personnel identify and collect valuable materials from a stream. These cabins can be found anywhere within the system. Quality-control units are situated immediately upstream of an output collection unit. At a QC unit, personnel remove contaminant materials from the stream to improve the grade of the material flow into the output collection unit. More information about how we model manual stations can be found in Appendix A.

3. Model parameter estimation

In this section, we show how to use data from an existing MRF to estimate the separation parameters required in the computational model. Alternatively, one might obtain the separation parameters directly from the equipment manufacturers or from the research literature. However, such estimates, if available, usually reflect the performance of the sorting equipment under ideal conditions rather than the actual MRF operating environment. For this paper, we assume that we can obtain sample measurements of the composition of the internal waste streams in the MRF. We rely on the concurrent sampling of various waste streams within the MRF, rather than attempting to measure individually the performance of each sorting unit. To do the latter requires that the normal operations of the MRF be stopped, which is quite expensive to do. Hence we rely on samples which can obtained with minimal disruption to the operations. Nevertheless, the quality of the data can be undermined by the fact that: (i) the samples are taken at different points in time, and there may be different compositions of the input waste stream entering the facility at these times; (ii) the mass of the samples is small compared to the total mass flow of material processed in the system; (iii) some of the samples might be incomplete, with some streams not being measured.

Let T be the number of datasets available, where each data set corresponds to sample measurements of waste streams at a subset of the sorting and output units of the MRF done with respect to the same input stream. We denote the set Z_t as the set of units sampled for dataset t. For each unit $j \in Z_t$ and each material m, we have a measurement $M^m_{j,t}$ of the mass flow that enters the system at unit j, and a measurement $F^m_{j,t}$ of the mass flow through or collected at unit j. For the optimization we require that at least one of the datasets is complete; i.e. Z_t contains measurements for all sorting units and all collection nodes.

We formulate a non-linear optimization model to determine the best fit that minimizes the squared error, where the error is the difference between the calculated (by the linear MRF model) and the measured mass flow rate. We solve the following optimization for each material type m (where we drop the superscript m for ease of presentation):

$$\min_{q,f} \sum_t \sum_{j \in Z_t} \beta_{j,t}(f_{j,t} - F_{j,t})^2 \tag{4}$$

$$\text{s.t.} f_{j,t} - \sum_{i|(i,j)\in T_t} f_{i,t} q_i^T - \sum_{i|(i,j)\in N_t} f_{i,t} q_i^N = M_{j,t} \;\forall\, j \in Z_t, \forall\, t \tag{5}$$

$$q_i^T + q_i^N = 1 \quad \forall\, i \in S \tag{6}$$

$$0 \le q_i^T \le 1; \quad 0 \le q_i^N \le 1 \quad \forall\, i \in S \tag{7}$$

$$f_{j,t} \ge 0 \quad \forall\, j \in \{Z_t, S\}, \forall\, t \tag{8}$$

N_t and T_t are respectively the arc sets for the non-target stream flows and the target stream flows for each sorting unit in the configuration of dataset t. The above formulation applies for binary units, i.e., units having only one target and one non-target stream, but can be easily extended to units with more than two outgoing streams.

For each material m, the decision variable q_i^T is the estimate of the separation parameter for sorting unit i, representing the fraction of the material that gets sorted into the target stream; $q_i^N = 1 - q_i^T$ is the fraction sorted into the non-target stream. The decision variable $f_{j,t}$ is the estimate of the mass flow through unit j for dataset t. The objective is to minimize the sum of the weighted squared errors of the mass flow estimates, where $\beta_{j,t}$ is the weight for the error terms for unit j for dataset t. Constraint (5) is a mass flow balance for each unit for each dataset. Constraints (6) and (7) ensure that the separation parameters are nonnegative and sum to one. We recommend setting the weight $\beta_{j,t}$ to give more importance (higher weight) to material measurements which are small fractions of the total mass at a measurement node unit, in order not to disregard them compared to materials measured in higher quantity (Testa, 2015). Finally, we solve the non-linear optimization problem with the iteration-point line-search filter method, using the Ipopt software package (Wächter and Biegler, 2006).

4. Model applications

The inputs for the mathematical model (2) for an MRF are estimates of the sorting matrix Q^m and input vector $\overline{\mu}^m$ for each material m. Given these inputs, we use (3) to predict the stationary flow rates f_i^m for each material at each node in the system configuration. We can use these flow rates to predict the performance of the MRF in terms of costs and revenues, and recovery measures.

4.1. Performance evaluation

For a user-defined configuration and set of inputs, the performance of an MRF can be measured with respect to different metrics: (i) overall plant efficiency, (ii) material recovery, (iii) material grade, and (iv) profit. To simplify the presentation, we assume that each material has a single target output unit, denoted by $i(m)$ for material m.

(i) The overall plant efficiency ε is a measure of how much of the incoming materials is correctly sorted, on a mass basis. We define the overall plant efficiency as:

$$\varepsilon = \frac{\sum_m f^m_{i(m)}}{\sum_m \mu_m} \tag{9}$$

where μ_m denotes the total input flow of material m to the MRF, and $f^m_{i(m)}$ is the amount that is correctly sorted.

(ii) Recovery R_m measures the fraction of material m that is collected at the desired output stream i.

$$R_m = \frac{f^m_{i(m)}}{\mu_m} \tag{10}$$

(iii) Grade measures the concentration of the target material m in the output stream i:

$$G_m = \frac{f^m_{i(m)}}{\sum_{m'} f^{m'}_{i(m)}} \tag{11}$$

(Testa, 2015; Wolf, 2011) discuss different ways to combine the different material grades or recoveries into single overall metrics.

(iv) Additionally, we can evaluate a particular MRF configuration in terms of the profit generated in one time period of operations. For instance, we might model profit as:

$$\pi = V_p + \sum_i V_i - (C_l + C_p + C_e + C_m) \tag{12}$$

Where C_p is cost of operating personnel, C_e is the energy cost of the machinery, and C_m is the cost of maintenance and cleaning. The cost of landfill, C_l, depends on landfill fee c_l \$/ton, and is given by $C_l = c_l \sum_{m\in M} f^m_l$. The revenue has two components. First is the

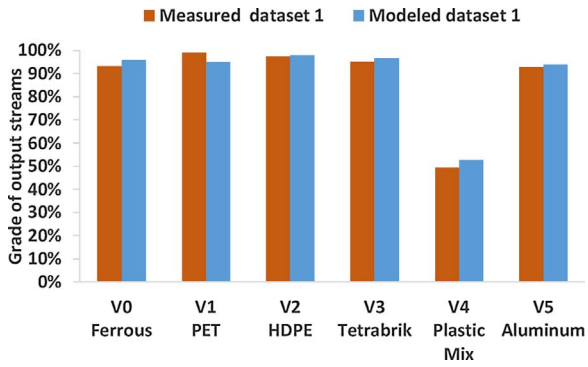

Fig. 3. Comparison of measured and estimated grades of output streams of LPRS with QC on.

revenue that is proportional to the amount of waste processed: $V_p = p_p \Sigma_{m \in M} \mu_m$, where $p_p$is the received processing fee ($/ton). The second is the revenue from the material collected at each output collection unit i: $V_i = p_i \sum_{m \in M} f_i^m$. Note that the price of output stream i, depends on whether the output concentration requirements are met. If not, a penalty function, based on the output grade, is applied to the nominal selling price. Hence for output stream $i(m)$, we model the price as:

$$p_{i(m)} = f(G_m) p_{i(m)}^{\text{nominal}} \tag{13}$$

where the function $f(G_m) = 1$ if the concentration requirements are met for material m; if not, then $f(G_m) < 1$ denotes the penalty as a function of the material grade.

4.2. Uncertainty and sensitivity analyses

The linear model of an MRF allows for rapid evaluation of different scenarios under the assumption of deterministic inputs and known separation parameters. However, it is often the case that these inputs are not well specified due to limited data for estimation and due to variation in the operating conditions. In this section, we discuss how uncertainty and variation in the parameters affects the performance of the model.

We have developed an uncertainty analysis to account for possible daily and seasonal variations in municipal solid waste composition. We view the inputs μ_m as being random variables, for which the user can define the uncertainty distribution for each material component. We use a Monte Carlo method to sample from the distributions and to determine distributions for performance metrics.

For the separation parameters, we may not have enough experimental data to determine their probability distribution. Rather we may only be able to estimate a range for each parameter. In this case we will use a sensitivity analysis (instead of a Monte-Carlo analysis) to gauge the influence of these parameter values on the MRF performance metrics, and to identify which parameter has the largest effect. There exist diverse computational methods for carrying out sensitivity analysis, including variance-based methods such as FAST and Sobol' series (Saltelli et al., 2010). However, as a preliminary step, which only focuses on a limited number of parameters, we use a *design of experiments* (DOE) method to structure the computational runs with different settings for the uncertain parameters. For the separation parameter of the target material of each sorting unit, we can find the average effect of increasing and decreasing its level, with the averaging done over all the runs of the different possible combinations of the levels of the remaining sorting units. We illustrate both the uncertainty and sensitivity analyses in the case-study in the next section.

5. Case-Study: LPRS in an MRF

5.1. Model formulation

We tested the MRF model with data from a material recovery facility operated by Ferrovial Services in the Ecoparque de Toledo, Spain. We modeled the light-packaging recovery section (LPRS) of the facility, which is the downstream portion of the facility. Much of the organic waste, paper, cardboard, glass and large objects have been removed by upstream processes before the waste stream enters the LPRS. The LPRS, depicted in Fig. 2, collects six valuable output streams (label V), and has two quality-control units (label QC) and eight mechanical sorting units (label U): a magnet, six detect-and-route units with NIR sensors, and an eddy-current separator which separate ferrous, plastics, and aluminum materials respectively.

The Ferrovial Services team performed characterizations of the LPRS output streams (V0, V1, V2, V3, V4 and V5 in Fig. 2) as detailed in (Testa, 2015): the plant was emptied and then run (without operational QC units) for 30 min with a regular quantity of input; samples were then collected from each output stream and characterized by material type. Two such measurements of the output streams were conducted in October 2014. From those datasets, we estimated the separation parameters (q_i^T and q_i^N in Fig. 2) of units U0 to U7 for each material using the estimation method in Section 3. These estimated parameters are listed in Appendix B (Tables B1–B4). When recirculation streams exist (in our case from units U4 and U7), measurements of those streams are necessary in addition to the output streams, to form a complete dataset (dataset 2 in Fig. 2).

In June of 2015, Ferrovial Services characterized samples from both the input and output of the LPRS. To test our model and estimated separation parameters, we used the measured LPRS input composition from June 2015 as model input, and compared the predicted grades of the output streams to the measured ones from June 2015. As shown in Fig. 3, the predicted grades are within 4% of the measured ones.

The output streams, except for the plastic mix (PP + Other Plastics) in stream V4, are baled and sold to recyclers. In the future the plastic mix will be processed into refuse-derived fuel (RDF) at the MRF. In our calculations, we assume each output stream selling price, $p_{i(m)}^{\text{nominal}}$, is broken down into a market price and a recovery-based subsidy as detailed in Appendix C. We furthermore assume the penalty function of Eq. (13) to depend on Ecoembes grade requirements (Table C2) and to be of the following form, based on the U.S. secondary materials' market price analysis detailed in (Wolf, 2011):

$$f(G_m) = \begin{cases} 1 & \text{if } G_m \geq G_m^{\text{required}} \\ (2G_m - G_m^{\text{required}})/G_m^{\text{required}} & \text{if } G_m^{\text{required}} > G_m > 0.5 \\ 0 & \text{otherwise} \end{cases} \tag{14}$$

5.2. Evaluation mode

To illustrate the application of our modeling tool, we evaluate the LPRS configuration using a typical input material composition, shown in Fig. 4, inferred from sample measurements done in October 2014. We note that there can be a large variation in the input composition can exist depending on the demographics of the municipality served by the MRF as well as the season, as shown by data collected by (Metin et al., 2003).

Our evaluation enables the determination of the grade and recovery for each valuable output stream, as shown in Fig. 5. The recovery of each valuable output material is above 90% except for aluminum; the grade of each output stream is above 90% except for plastic mix.

While the profit of the LPRS will increase with the recovery rate for each material, this need not be the case with the material grade. In particular, once the concentration requirement in Eq. (14) is met, there is no additional economic gain from improving the grade.

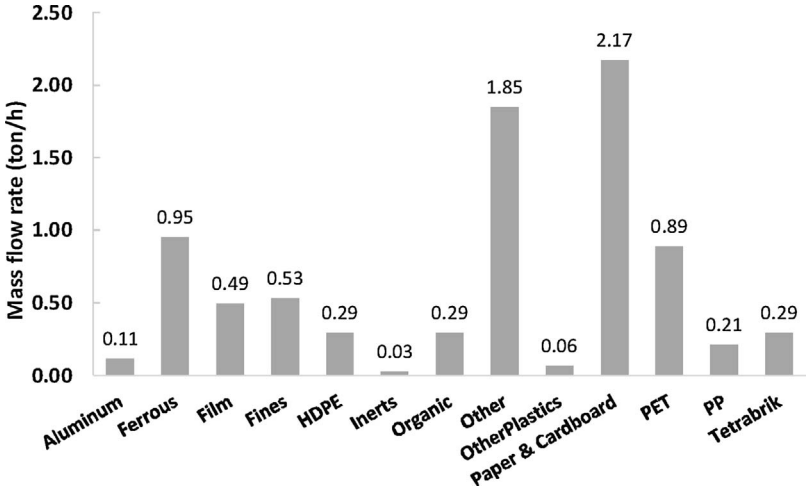

Fig. 4. Sample material composition in input stream to LPRS.

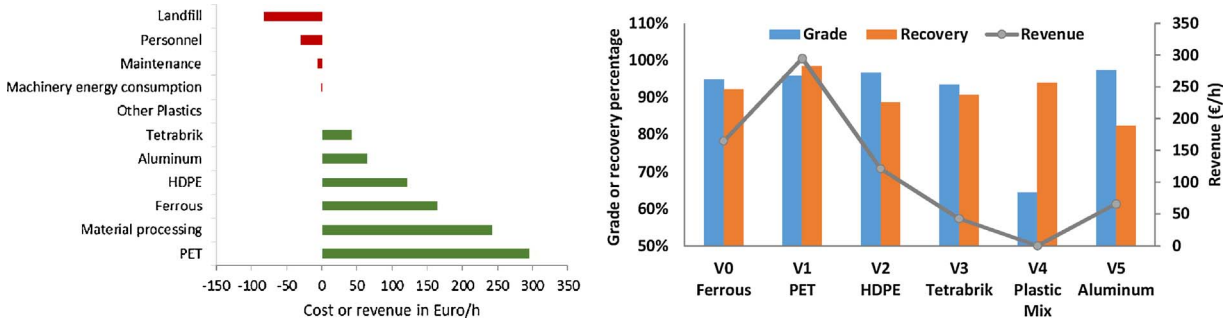

Fig. 5. Simulation results using input composition in Fig. 4: (i) breakdown of costs (in black) and revenues (in gray) and (ii) output streams' grade and recovery rate.

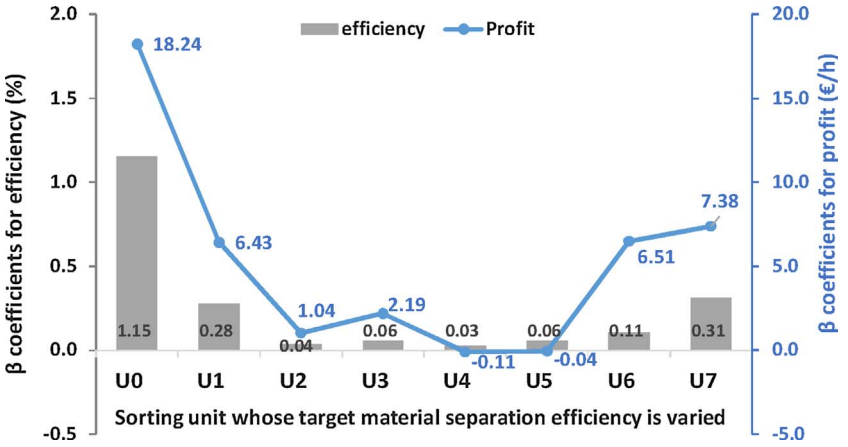

Fig. 6. Sensitivity analysis of varying sorting units' target material(s) separation efficiency on: (primary axis) net profit π, (secondary axis) overall plant efficiency ε.

The evaluation also enables us to analyze the economic performance of the MRF configuration. Costs C_l, C_p, C_e, C_m are respectively 82, 29, 1 and 7 €/ton (Fig. 5(i)). We observe that the largest cost comes from landfill fees charged at a rate of 15.49 €/ton. Output-stream revenues are shown on the secondary axis in Fig. 5(ii). Note that revenue from processing is significant (26% of revenues) as the MRF facility is remunerated at a rate of p_p = 29.74€/ton of total input. This results in a net profit of 770 €/h for the input composition used.

We can compare our results to those for an e-waste MRF (Kang and Schoenung, 2006). We did not include the transportation costs to the MRF or to landfill. For comparison, transportation accounted for 14% of the cost at the e-waste MRF. Additionally, their largest cost (30%) came from CRT recycling as it is illegal to landfill CRT in California. Their second largest cost was labor (28%), similar to the labor cost fraction in our case-study. Finally, we note that most of their revenues come from fees charged to customers (59%), while only 28% comes from metals recovery, and 7% from plastic recovery (Kang and Schoenung, 2006); in our case, the processing fee revenue received by the MRF (26%) is smaller than metals recovery (25%) and plastic recovery (49%) revenues.

The overall sorting performance of this particular LPRS configuration can be summarized by an efficiency (Eq. (9)) of 95.0%. While the metrics of profit and efficiency may not be useful in isolation, they can be used for comparing performance of different input compositions or different configuration designs. For instance, Testa (2015) used a genetic algorithm approach to generate different configurations and select those with the highest performance metrics. In addition, an MRF manager can use the evaluation model to test various strategies for responding to changes in scrap market prices or scrap grade specifications. These strategies can include adding labor for output quality

control or for increased screening of inputs, as well as modifying the operational controls on sortation equipment so as to improve their separation efficiencies.

5.3. Uncertainty analysis

The historical data for mass entering the LPRS system are from samples taken at 9 different times throughout the year, hence 9 observations. Using their minimum, maximum and mean values (Table D1), we can define an uncertainty distribution for each material input mass. Due to the limited number of observations, we assume either a uniform or triangular distribution.

We use the Monte Carlo method to sample from the distributions and to determine the resulting probability distributions for performance metrics and each output-stream revenue. This uncertainty analysis shows a unimodal distribution for profit (mean: 854 €/h, standard deviation: 77 €/h) and efficiency (mean: 92.6%, standard deviation: 1.2%), and a more uniform-like distribution for some of the output-streams' revenues. Histograms and goodness-of-fit tests of these distributions can be found in the Appendix D.

The uncertainty analysis allows us to generate distributions of performance metrics. For instance, the distribution of projected revenues can be used by MRF managers for long-term planning such as annual budgeting purposes while incorporating the effect of variation in waste composition of the MRF feed throughout a year. Moreover, during the configuration design phase, one can run several scenarios for each possible configuration to determine the relative robustness of the configurations to the variability in the input composition. Another possible usage of uncertainty analysis is to examine the impact of scrap price variation, as done in Li et al., 2011.

5.4. Sensitivity analysis

We conduct a sensitivity analysis using DOE to investigate the influence of the separation parameters of the sorting units within the LPRS system on its performance. We consider 3 levels for the separation parameters of the target material(s) for each of the 8 sorting units in the configuration: (i) low at 78%, (ii) medium at 88%, (iii) high at 98%. These 3 levels reflect the range of variation in measured separation efficiencies observed during experimental runs on standalone machines of the magnet, eddy-current and NIR, where operating settings (magnet belt height, rotor speed and material selectivity respectively) were changed (Raymond, 2017). With a simple factorial design of the computational experiment, this results in $3^8 = 6561$ runs, each with a different combination of target-material separation parameters for the 8 sorting units. Note that a sorting unit can have more than 1 target material: U1 targets PET and Tetrabrik, while U7 targets PET, Tetrabrik, HDPE, and plastic mix.

We consider the main effects of these factors on our model outputs, in particular on the net profit, on the overall plant efficiency, and on specific revenues from the collected materials. The main effect, i.e. the first-order influence, of each uncertain parameter on the outputs is measured using linear regression of the following form, for n uncertain parameters:

$$\hat{y} = \beta_0 + \beta_1 x_1 + \beta_2 x_2 + \ldots + \beta_n x_n \quad (15)$$

Where $\hat{y}$ is the predicted output, x_i is the level (-1 for lowest, 0 for medium and $+1$ for highest efficiency) of the i^{th} uncertain parameter, β_i is the regression coefficient indicating the level of influence of x_i.

For the LPRS, we use the input composition in Fig. 4, with $n = 8$. For profit as the predicted output, $\beta_0 = 781$ €/h, while for efficiency, $\beta_0 = 93\%$. The other coefficients are given in Fig. 6, which shows us the relative influence of improving the separation efficiency of each sorting unit on the net profit and overall plant efficiency. The sorting units that have the highest positive influence are U0, U6, U7 and U1. We can expect the influence of the units that are upstream in the LPRS configuration (U0, U1) to be more important. The influence of U6 on profit is due to the high selling price of aluminum. U7, which feeds a recirculation loop and has multiple target materials, also has comparable influence. Additionally, the target materials' input flow rate has an impact on the sorting unit's individual influence on efficiency, while both the input flow rate and the output streams' selling price influence profit. Note that U4 and U5 have a slightly negative influence on profit: increasing their target material separation efficiency (Tetrabrik and PP + OtherPlastics respectively) decreases profit slightly. This can be attributed to: (i) the target materials having a small input flow rate and low selling price; (ii) the uncollected target materials being recirculated back to the rest of the configuration to be distributed to the other output collection units, by an amount small enough to increase their output mass but still keep the contaminants within the limits of concentration requirements. Please refer to Appendix E for more details on which specific revenue streams contribute to the influence on profit from the LPRS.

This sensitivity analysis can highlight the most influential parameters on the MRF performance. As such, it can be useful to MRF managers for informing their investment and operating decisions. For instance, based on the sensitivity analysis for our case-study, the MRF managers could be advised to concentrate improvement efforts at the specific sorting units U0 and U7, as this would have the most impact on the performance metrics. Alternatively, the managers might decide to invest in more efficient machinery, balancing the projected increase in profit (from increased material recovery and revenue) with the incurred capital costs and operating costs.

6. Conclusion and future works

We tested the network flow model on part of an existing MRF configuration and obtained reasonable predicted performance. Moreover, we showed possible applications of the model through uncertainty and sensitivity analyses. The former evaluates the impact from uncertainty in input material composition on the performance; the latter shows the sensitivity of the configuration performance to the separation efficiency of individual sorting units. We found that the impact of unit separation efficiencies on the plant performance depends on its configuration design: the marginal benefit of improving the separation efficiency of a unit is greater if it is more upstream of the valuable output, and if it leads to a recirculation loop. Future work will look at the impact of recirculation loops and different sequences of units on plant performance, in terms of the trade-off between recovery rate and grade. Additionally, we observed that improving grade does not necessarily translate to maximizing profit, as there is no price premium from exceeding the grade requirements.

Currently, we assume that the estimated separation efficiencies are independent of the input composition or flow rate. In future work, one might examine how the separation parameters depend on both input composition and rate. Additionally, one might investigate the dependence between different material streams for a given fixed total flow rate, as the current model assumes independence.

Acknowledgments

The authors give their sincere thanks to Ferrovial, the sponsor of this project and especially to the Innovation and Processes department of Ferrovial, the Centre of Excellence for Environment of Ferrovial Services and the Ecoparque de Toledo teams.

Appendix A. Manual sorting

A manual station can be a hand-sorting cabin or a quality-control unit. For each type of manual station we assume that each manual sorter has a recovery efficiency r_{worker}, which is a function of the actual flow and predetermined flow thresholds (Testa, 2015; UNEP, 2005). r_{worker} is thus the

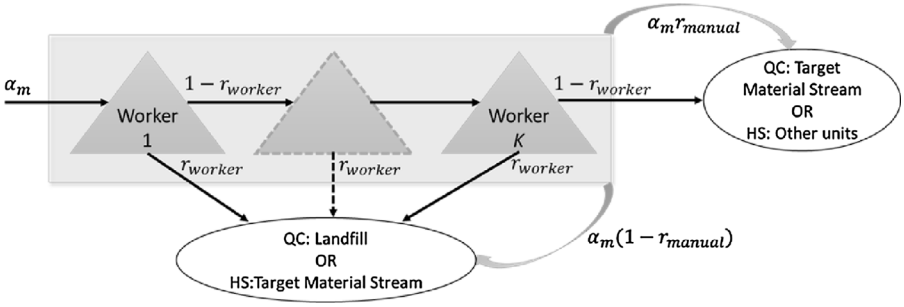

Fig. A1. Representation of a HS or QC unit, adapted from (Testa, 2015).

fraction of the target material that is recovered by the sorter. When the station has more than one sorter, the recovery efficiency is a geometric sum of their individual efficiencies. Hence, the overall recovery efficiency $r_{manual}$for a target material for a unit with K sorters is given by (Testa, 2015):

$$r_{manual} = \sum_{i=0}^{K} r_{worker}(1 - r_{worker})^i \quad (A.1)$$

Appendix B. LPRS case-study separation parameter estimates

Tables B1–B4 show the estimated separation parameters of the 8 sorting units in the Light Packaging Recovery System (LPRS). The parameters

Table B1
Separation parameters of unit U0 and unit U1.

Magnet − U0		
Material	End node	
	V0	U1
Aluminum	0.07%	99.93%
Ferrous	95.10%	4.90%
Film	1.44%	98.56%
Glass	0.22%	99.78%
HDPE	0.05%	99.95%
Inert	0.00%	100.00%
Other	1.47%	98.54%
PET	0.12%	99.88%
PP	0.24%	99.76%
Tetrabrik	0.16%	99.84%
Fines	1.42%	98.58%
Organic	0.02%	99.98%
Other Plastics	0.31%	99.70%
Paper & Cardboard	0.07%	99.93%
NIR - U1		
	U2	U3
Aluminum	3.93%	96.07%
Ferrous	0.00%	100.00%
Film	9.13%	90.87%
Glass	21.29%	78.71%
HDPE	0.24%	99.76%
Inert	0.58%	99.42%
Other	1.40%	98.60%
PET	86.23%	13.77%
PP	5.74%	94.26%
Tetrabrik	71.94%	28.06%
Fines	1.30%	98.70%
Organic	0.04%	99.96%
Other Plastics	6.95%	93.05%
Paper & Cardboard	4.67%	95.33%

Table B2
Separation Parameters of units U2 and U3.

NIR − U2		
Material	End node	
	U4	V1
Aluminum	95.26%	4.74%
Ferrous	66.25%	33.75%
Film	86.84%	13.16%
Glass	98.97%	1.03%
HDPE	79.34%	20.66%
Inert	99.93%	0.07%
Other	68.25%	31.75%
PET	6.81%	93.19%
PP	88.12%	11.88%
Tetrabrik	96.25%	3.75%
Fines	60.47%	39.53%
Organic	99.95%	0.05%
Other Plastics	89.26%	10.74%
Paper & Cardboard	95.15%	4.85%
NIR − U3		
	U5	V2
Aluminum	99.93%	0.07%
Ferrous	100.00%	0.00%
Film	93.27%	6.73%
Glass	99.72%	0.28%
HDPE	28.71%	71.29%
Inert	100.00%	0.00%
Other	99.72%	0.28%
PET	99.68%	0.32%
PP	99.59%	0.42%
Tetrabrik	99.73%	0.27%
Fines	99.95%	0.05%
Organic	100.00%	0.00%
Other Plastics	99.07%	0.93%
Paper & Cardboard	99.99%	0.01%

Table B3
Separation parameters of unit U4 and unit U5.

NIR − U4 Material	End node	
	U0	V3
Aluminum	96.79%	3.21%
Ferrous	49.83%	50.17%
Film	95.39%	4.61%
Glass	98.96%	1.04%
HDPE	72.29%	27.71%
Inert	99.93%	0.07%
Other	84.74%	15.26%
PET	99.31%	0.69%
PP	95.44%	4.56%
Tetrabrik	3.71%	96.29%
Fines	88.76%	11.24%
Organic	91.02%	8.98%
Other Plastics	92.30%	7.70%
Paper & Cardboard	85.32%	14.68%
NIR − U5		
	U6	V4
Aluminum	97.90%	2.10%
Ferrous	99.83%	0.17%
Film	78.21%	21.79%
Glass	78.19%	21.81%
HDPE	99.20%	0.81%

Table B3 (*continued*)

NIR – U5		
	U6	V4
Inert	100.00%	0.00%
Other	96.27%	3.73%
PET	99.51%	0.49%
PP	26.40%	73.60%
Tetrabrik	99.73%	0.27%
Fines	99.77%	0.24%
Organic	99.94%	0.06%
Other Plastics	25.55%	74.45%
Paper & Cardboard	99.68%	0.32%

Table B4
Separation Parameters of units U6 and U7.

NIR – U6		
Material	End node	
	U7	V5
Aluminum	15.37%	84.63%
Ferrous	100.00%	0.00%
Film	99.92%	0.08%
Glass	23.85%	76.15%
HDPE	99.74%	0.26%
Inert	100.00%	0.00%
Other	99.58%	0.42%
PET	99.77%	0.23%
PP	99.04%	0.96%
Tetrabrik	95.15%	4.85%
Fines	99.90%	0.11%
Organic	99.95%	0.05%
Other Plastics	99.17%	0.83%
Paper & Cardboard	99.96%	0.04%

NIR – U7		
	U0	L0
Aluminum	28.98%	71.02%
Ferrous	0.00%	100.00%
Film	38.82%	61.18%
Glass	98.50%	1.50%
HDPE	71.06%	28.94%
Inert	0.00%	100.00%
Other	0.88%	99.12%
PET	91.12%	8.88%
PP	87.66%	12.34%
Tetrabrik	94.98%	5.02%
Fines	0.97%	99.03%
Organic	0.02%	99.98%
Other Plastics	94.14%	5.86%
Paper & Cardboard	3.27%	96.73%

were estimated from 2 datasets (see Fig. 2) using the model separation method described in Section 3.

Appendix C. Material selling price breakdown

For each valuable material, its selling price can be broken down into a market price and a recovery-based subsidy as shown in Table C1. This Ecoembes subsidy can be high or low, depending on whether the output stream meets the Spanish recycling industry standards, i.e., whether the recovered fraction of the total mass of processed valuable material m, is above a predefined Ecoembes threshold value or not. Note that Ecoembes is a non-profit public limited company in Spain in charge of an integrated management system for waste collection and recovery (Ecoembes, n.d.). Additionally, Ecoembes imposes grade requirements on the collected output streams as in Table C2.

Table C1
Selling price breakdown of material output streams as of May 2015 with either low or high Ecoembes subsidy.

Valuable Material (Output Stream)	Market Price	Ecoembes subsidy	
		Low	High
Ferrous (V0)	170	6	9
PET (V1)	170	118	150
HDPE (V2)	360	45	90
Tetrabrik (V3)	7	150	150
Plastic Mix (V4)	0	0	0
Aluminum (V5)	700	9	27

Table C2
Ecoembes concentration requirements for valuable output streams.

Output	Materials in Output	Concentration	
		Min	Max
Aluminum	Aluminum	0.80	1.00
	Ferrous	0.00	0.00
	HDPE; PET; PP; Film; OtherPlastics; Tetrabrik; PaperAndCardboard	0.00	0.04
	HDPE; PET; PP;Film; OtherPlastics	0.00	0.02
	PaperAndCardboard	0.00	0.02
	Tetrabrik	0.00	0.02
	Fines; Other; Organic; Glass; Inerts	0.00	0.06
Ferrous	Ferrous	0.80	1.00
HDPE	HDPE	0.85	1.00
	PET; PP; OtherPlastics; Film	0.00	0.10
	Ferrous; Aluminum	0.00	0.01
	PaperAndCardboard; Tetrabrik; Fines; Organic; Glass; Inerts; Other	0.00	0.05
PP + OtherPlastics	PP; OtherPlastics	0.00	1.00
APET	PET	0.92	1.00
	Ferrous; Aluminum	0.00	0.01
	HDPE; PP; OtherPlastics; Film; Fines; Organic; PaperAndCardboard; Tetrabrik; Glass; Inerts; Other	0.00	0.07
Tetrabrik	Tetrabrik	0.95	1.00
	HDPE; PET; Ferrous; Aluminum	0.00	0.03
	Fines; Organic; PaperAndCardboard; OtherPlastics; PP; Film; Glass; Inerts; Other	0.00	0.02
Paper and Cardboard	PaperAndCardboard	0.97	1.00

Appendix D. Monte-Carlo generated distributions

Table D1 shows the input mass fraction variation within data from 9 historical datasets of measurements from the input flow to the Light Packaging Recovery System (LPRS).

Fig. D1 shows the resulting distributions for profit and overall plant efficiency from the Monte-Carlo analysis with uncertainty variation in the input parameters in Table D1. Using Chi-square goodness-of-fit test, we accept the null hypothesis that the profit distribution is normal with a *p*-value

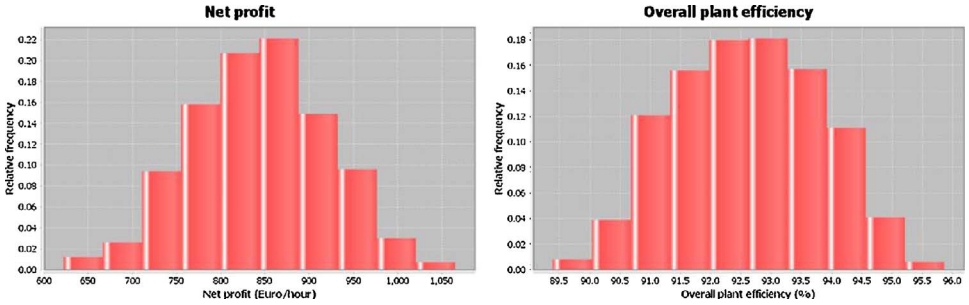

Fig. D1. Sample results' probability distributions for the LPRS configuration and uniformly-distributed input material mass for: (left) net profit π, (right) overall plant efficiency ε.

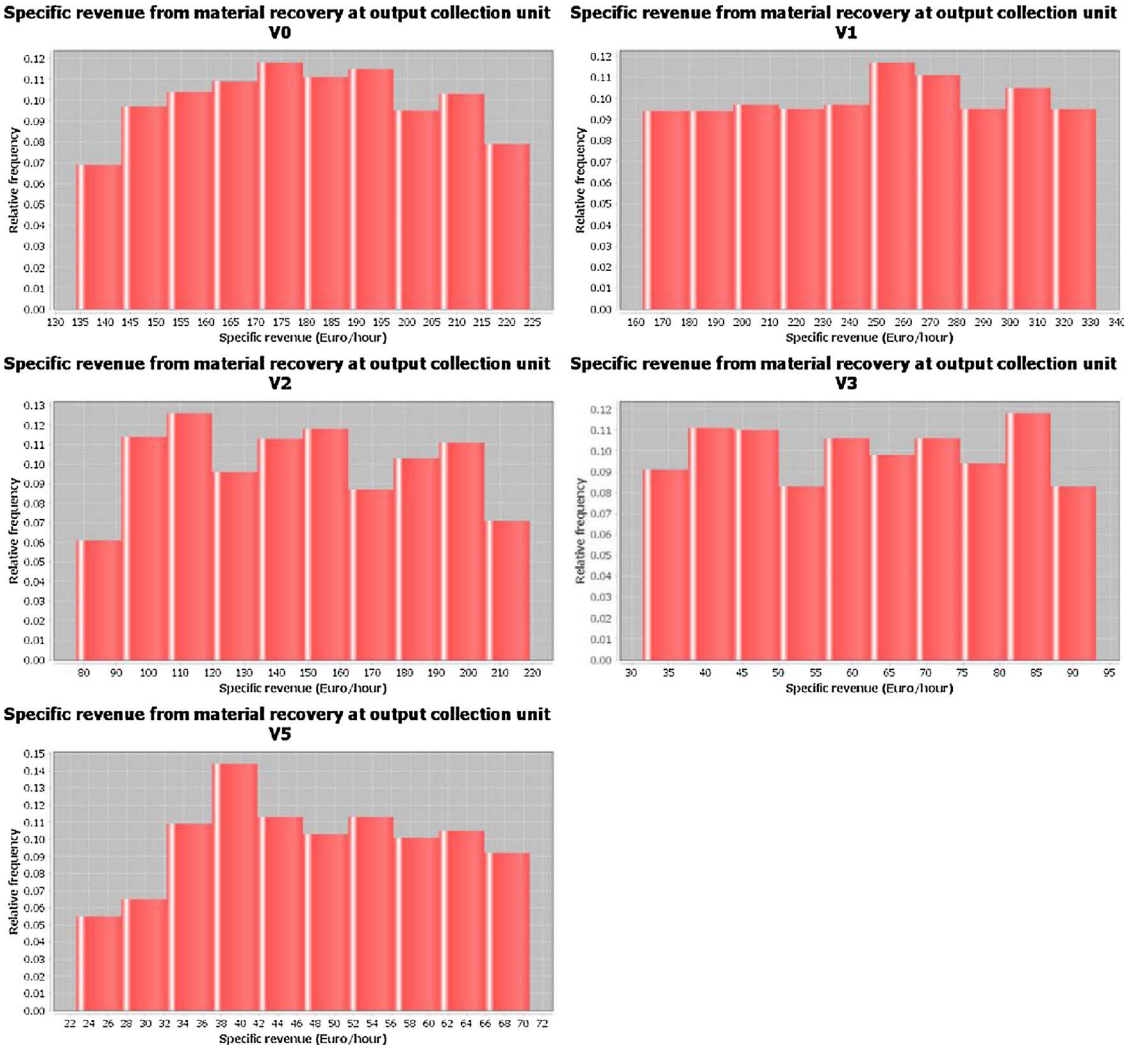

Fig. D2. Sample results' probability distributions for the LPRS configuration and uniformly-distributed input material mass for specific revenues from output −streams V0-V5.

of 0.40 for profit.

Fig. D2 shows resulting distributions in specific revenues from each of the output streams of the LPRS. Specific revenues from V1, V2, V3 and V5 have respectively a mean of 180, 248, 148, 62, 48 €/h, and standard deviation of 24, 48, 38, 17, 13 €/h. Using Chi-square goodness-of-fit test, we accept the null hypothesis that V1 and V3 specific revenue distribution is uniform with a *p*-value of 0.74 and 0.16 respectively (*p*-values for the other distributions were less than 0.05). Note that there is no revenue from plastic mix (V4), as this output-stream is not yet sold as RDF.

Table D1
Sample input mass fraction variation (LPRS system) used in Monte-Carlo analysis from 9 historical datasets.

Materials	Percentage of total input composition by mass		
	Lower Bound	Mean	Upper Bound
Aluminum	0.45%	1.09%	1.38%
Ferrous	9.36%	11.36%	15.65%
Film	4.97%	12.24%	24.04%
Fines	0.15%	1.85%	6.48%
Glass	0.00%	0.35%	1.38%
HDPE	2.21%	3.76%	6.28%
Inerts	0.31%	3.72%	12.18%
Organic	3.55%	7.69%	22.02%
Other	21.53%	27.18%	39.31%
OtherPlastics	0.13%	0.63%	1.61%
PaperAndCardboard	6.23%	11.25%	26.59%
PET	6.05%	9.78%	12.07%
PP	2.27%	4.52%	6.95%
Tetrabrik	2.74%	4.58%	7.73%

Appendix E. Sensitivity analysis with respect to material revenues

To investigate which revenue streams contribute to the influence on profit from the LPRS, we examine the influence of the sorting units on the specific revenues from each collection unit (Fig. E1). Looking at the Ferrous (V0) revenue coefficient line chart, we observe that the only major positive influence on Ferrous revenue is from increasing the separation efficiency in U0. On the other hand, increasing the target material separation efficiency in U1, U2, and U7 has a positive influence on PET (V1) revenue, while increasing it in U4 actually has a slightly negative influence, due to

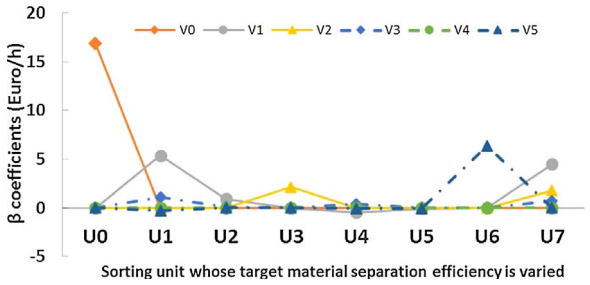

Fig. E1. Sensitivity analysis of varying sorting units' target material(s) separation efficiency on V_z, the revenue for output-stream z, where z = {V0, V1, V2, V3, V4, V5}.

contamination inflating V1 revenue, as discussed above. U1 has more influence than U2 because U1 also targets PET and is upstream of U2. It is interesting to note that U7, even though it is downstream of U2, has a higher influence than U2; this is because U7 determines how much PET gets recirculated and eventually ends up collected at V1. Similarly for HDPE (V2) revenue, U3 (which sorts for HDPE to V2) and U7 have the most influence. Again, recall that NIR U7 has HDPE as a target material. As expected for aluminum revenue, U6 (which sorts for aluminum) has the major positive influence.

References

Antmann, E.D., Shi, X., Celik, N., Dai, Y., 2013. Continuous-discrete simulation-based decision making framework for solid waste management and recycling programs. Comput. Ind. Eng. 65, 438–454. http://dx.doi.org/10.1016/j.cie.2013.03.010.

Braam, B.C., Van Der Valk, H.J.L., Dalmijn, W.L., 1988. Eddy-current separation by permanent magnets part II: Rotating disc separators. Resour. Conserv. Recycl. 1, 3–17. http://dx.doi.org/10.1016/0921-3449(88)90003-1.

Chang, N.-B., Pires, A., 2015. Sustainable Solid Waste Management: A Systems Engineering Approach. John Wiley & Sons, Inc., Hoboken, NJ, USA. http://dx.doi.org/10.1002/9781119035848.

Chang, N.-B., Davila, E., Dyson, B., Brown, R., 2005. Optimal design for sustainable development of a material recovery facility in a fast-growing urban setting. Waste Manage. 25, 833–846. http://dx.doi.org/10.1016/j.wasman.2004.12.017.

Dahmus, J.B., Gutowski, T.G., 2007. What gets recycled: an information theory based model for product recycling. Environ. Sci. Technol. 41, 7543–7550. http://dx.doi.org/10.1021/es062254b.

Diaz, L.F., Savage, G.M., Golueke, C.G., 1982. Resource Recovery from Municipal Solid Wastes. CRC.

Ecoembes, n.d. About Ecoembes: Who are we? [WWW Document]. URL https://www.ecoembes.com/en/citizens/ecoembes/who-are-we (accessed 4.12.17).

Gaustad, G., Olivetti, E., Kirchain, R., 2012. Improving aluminum recycling: a survey of sorting and impurity removal technologies. Resour. Conserv. Recycl. 58, 79–87. http://dx.doi.org/10.1016/j.resconrec.2011.10.010.

Gu, F., Ma, B., Guo, J., Summers, P.A., Hall, P., 2017. Internet of things and big data as potential solutions to the problems in waste electrical and electronic equipment management: an exploratory study. Waste Manage. 68, 434–448. http://dx.doi.org/10.1016/j.wasman.2017.07.037.

Gutowski, T., Dahmus, J., Albino, D., Branham, M., 2007. Bayesian material separation model with applications to recycling. IEEE Int. Symp. Electron. Environ. 233–238. http://dx.doi.org/10.1109/ISEE.2007.369400.

Gutowski, T., Wolf, M.I., Dahmus, J., Albino, D., 2008. Analysis of Recycling Systems. In: Proc. 2008 NSF Eng. Res. Innov. Conf. Knoxville. Tennessee.

Hershaft, A., 1972. Solid waste treatment technology. Environ. Sci. Technol. 6, 412–421. http://dx.doi.org/10.1021/es60064a009.

Huang, G.H., Linton, J.D., Yeomans, J.S., Yoogalingam, R., 2005. Policy planning under uncertainty: efficient starting populations for simulation-optimization methods applied to municipal solid waste management. J. Environ. Manage. 77, 22–34. http://dx.doi.org/10.1016/j.jenvman.2005.02.008.

Huang, J., Pretz, T., Bian, Z., 2010. Intelligent solid waste processing using optical sensor based sorting technology. 2010, 3rd International Congress on Image and Signal Processing. IEEE 1657–1661. http://dx.doi.org/10.1109/CISP.2010.5647729.

Kang, H.Y., Schoenung, J.M., 2006. Economic analysis of electronic waste recycling: modeling the cost and revenue of a materials recovery facility in California. Environ. Sci. Technol. 40, 1672–1680. http://dx.doi.org/10.1021/es0503783.

Kirkeby, J.T., Birgisdottir, H., Hansen, T.L., Christensen, T.H., Bhander, G.S., Hauschild, M., 2006. Environmental assessment of solid waste systems and technologies: EASEWASTE. Waste Manage. Res. 24, 3–15. http://dx.doi.org/10.1177/0734242X06062580.

Li, P., Dahmus, J., Guldberg, S., Riddervold, H.O., Kirchain, R., 2011. How much sorting is enough: identifying economic and scrap-reuse benefits of sorting technologies. J. Ind. Ecol. 15, 743–759. http://dx.doi.org/10.1111/j.1530-9290.2011.00365.x.

Mckeon, T., Luttrel, G.H., 2012. Optimization of multistage circuits for gravity concentration of heavy mineral sands. Miner. Metall. Process. 29, 1–5.

Metin, E., Eröztürk, A., Neyim, C., 2003. Solid waste management practices and review of recovery and recycling operations in Turkey. Waste Manage. 23, 425–432. http://dx.doi.org/10.1016/S0956-053X(03)00070-9.

Milios, L., Reichel, A., 2013. Municipal Waste Management in Spain-European Environment Agency.

Noble, A., Luttrell, G.H., 2014a. Value-based objective functions applied to circuit analysis. Sme 32.

Noble, A., Luttrell, G.H., 2014b. The matrix reduction algorithm for solving separation circuits. Miner. Eng. 64, 97–108. http://dx.doi.org/10.1016/j.mineng.2014.05.024.

Palmer, J.R., 1999. Concept Design and Optimization of MSW Management System. Air Force Institute of Technology Air Universityhttp://dx.doi.org/10.1017/CBO9781107415324.004.

Ragaert, K., Delva, L., Van Geem, K., 2017. Mechanical and chemical recycling of solid plastic waste. Waste Manage. 69, 24–58. http://dx.doi.org/10.1016/j.wasman.2017.07.044.

Raymond, A.G., 2017. Modeling of Material Recovery Facility Performance with Applications for Life Cycle Assessment (SM Thesis). Massachusetts Institute of Technology.

Rigamonti, L., Grosso, M., Møller, J., Martinez Sanchez, V., Magnani, S., Christensen, T.H., 2014. Environmental evaluation of plastic waste management scenarios. Resour. Conserv. Recycl. 85, 42–53. http://dx.doi.org/10.1016/j.resconrec.2013.12.012.

Saltelli, A., Annoni, P., Azzini, I., Campolongo, F., Ratto, M., Tarantola, S., 2010. Variance based sensitivity analysis of model output. Design and estimator for the total sensitivity index. Comput. Phys. Commun. 181, 259–270. http://dx.doi.org/10.1016/j.cpc.2009.09.018.

Schloemann, E., 1982. Eddy-current techniques for segregating nonferrous metals from waste. Conserv. Recycl. 5, 149–162. http://dx.doi.org/10.1016/0361-3658(82)90024-8.

Shi, X., Thanos, A.E., Celik, N., 2014. Multi-objective agent-based modeling of single-stream recycling programs. Resour. Conserv. Recycl. 92, 190–205. http://dx.doi.org/10.1016/j.resconrec.2014.07.002.

Shonfield, P., 2008. LCA of Management Options for Mixed Waste Plastics. Waste Resource Action Programme WRAP, London.

Stressel, R., 2012. Recycling and Resource Recovery Engineering. Springerhttp://dx.doi.org/10.1017/CBO9781107415324.004.

Testa, M., 2015. Modeling and Design of Material Recovery Facilities: Genetic Algorithm Approach. Operations Research Center, Massachusetts Institute of Technology (SM thesis).

UNEP, 2005. Chapter vi. Materials Recovery and Recycling.

Van Den Broek, W.H.A.M., Wienke, D., Melssen, W.J., Feldhoff, R., Huth-Fehre, T., Kantimm, T., Buydens, L.M.C., 1997. Application of a spectroscopic infrared focal plane array sensor for on-line identification of plastic waste. Appl. Spectrosc. 51,

856–865.
Vanegas, P., Peeters, J.R., Dewulf, W., Cattrysse, D., Duflou, J.R., 2015. Improving resource efficiency through recycling modelling: a case study for LCD TVs. Procedia CIRP 26, 601–606. http://dx.doi.org/10.1016/j.procir.2014.07.089.
Wächter, A., Biegler, L.T., 2006. IPOPT: On the Implementation of an Interior-point Filter Line-search Algorithm for Large-scale Nonlinear Programming Mathematical Programming. http://dx.doi.org/10.1007/s10107-004-0559-y.
Wolf, M.I., Colledani, M., Gershwin, S.B., Gutowski, T.G., 2013. A network flow model for the performance evaluation and design of material separation systems for recycling. IEEE Trans. Autom. Sci. Eng. 10.
Wolf, M., 2011. Modeling and Design of Material Separation Systems with Applications to Recycling. Mechancial Engineering, Massachusetts Institute of Technology (Ph.D. thesis).